Spatial weak-light ring soliton in self-assembled quantum dots*

Chen Qiu-Cheng(陈秋成)†

Department of Physics and Electronic Information Science, Hengyang Normal University, Hengyang 421008, *China*

(Received 19 January 2014; revised manuscript received 16 May 2014; published online 10 October 2014)

By using semiclassical theory combined with multiple-scale method, we analytically study the linear absorption and the nonlinear dynamical properties in a lifetime broadened Λ-type three-level self-assembled quantum dots. It is found that this system can exhibit the transparency, and the width of the transparency window becomes wider with the increase of control light field. Interestingly, a weak probe light beam can form spatial weak-light dark solitons. When it propagates along the axial direction, the soliton will transform into a steady spatial weak-light ring dark soltion. In addition, the stability of two-dimensional spatial optical solitons is testified numerically.

Keywords: spatial weak-light ring dark soliton, electromagnetically induced transparency, self-assembled quantum dots

PACS: 42.65.Tg, 42.50.Gy, 02.90.+P **DOI:** 10.1088/1674-1056/23/12/124212

1. Introduction

Spatial optical solitons are localized optical beams that form in an optical medium when the combined effects of refractive nonlinearity and beam diffraction can compensate for each other. It is promising for practical and potential applications in optical signal processing, optical networks, and optical telecommunication.[1–4] The previous research on spatial optical solitons is limited to conventional nonlinear mediums.[3,4] In conventional nonlinear media, such as two-level atomic medium,[4] a large nonlinear refractive index is always associated with large absorption, which is a basic limitation to producing solitons at very low light intensities.[1–4] Fortunately, electromagnetically induced transparency (EIT) has been found to lead to a great enhancement in nonlinear effects even under a weak driving optical pulsed field.[5–13] So, the spatial optical solitons in EIT media, such as waveguide, atomic media, and quantum well, have received increasing attention.[14–27] Among these media, the atomic system plays a leading role in studying the spatial optical pulse with vanishing absorption solitons. However, one potential shortcoming of the atomic system is that it cannot be conveniently used in devices with good scalability. The basic concept of forming spatial optical solitons in an atomic system can also be applied to optical processes in the fields of the semiconductors quantum dots (QDs) and quantum wells. For example, epitaxially grown single QDs feature discrete spectrally sharp optical transitions, arising from their atomic-like energy level structures. In particular, the mature semiconductor manufacturing technologies in addition to the molecule beam epitaxy growth technology highly promote the development of the semiconductor devices.[28,29]

In QDs as compared with quantum wells, coherence times are rather long, so the dots seem to be an optimal semiconducting medium for EIT. Various EIT processes have also been explored experimentally as well as theoretically in QDs.[28–33] For example, Villas *et al.*[30] found that it is possible to use Rabi oscillations to coherently control the electron tunneling in an asymmetric double QDs system. Yang *et al.*[31] also testified that the slow optical soliton pairs can form and stably propagate in semiconductor QDs with a four-level biexciton–exciton cascade configuration. She *et al.*[32] showed the temporal optical solitons can appear in a four-level quantum dot molecule system. To our knowledge, a classical EIT scheme is a three-level system in which two of the transitions, control and signal, are dipole-transition-allowed and the third, is the dipole transition-forbidden. Li *et al.*[33] put forward an efficient scheme for producing spatial weak infrared-light solitons based on interband transition in GaAs–Al–GaAs QD structures operating within optical communication wavelength band under a mechanism of EIT. Especially, Marcinkevičius *et al.*[34] observed a lifetime broadened Λ-type three-level self-assembled QDs in pump-probe experiment on a ten layer optically thin InGaAs/GaAs structure. However, for single QDs, there is little literature dealing with the physics properties of three-level quantum dots. This is a reason that a QD ensemble has a serious drawback, namely, the inhomogeneous broadening, which severely affects manifestation of EIT. Fortunately, in self-assembled QDs, the inhomogeneous broadening is typically 20 meV or more, which should be compared with an EIT window of about 1 meV. That is to say, a Λ-type three-level system has been realized experimentally in lifetime broadened self-assembled QDs.[34] As far as we know, there is little relevant theoretical work on exploring spatial solitons with weak-light intensity in the three-level QDs, which motivates us to

*Project supported by the Special Funds of the National Natural Science Foundation of China (Grant No. 11247313).

†Corresponding author. E-mail: chenqiucheng68@126.com

© 2014 Chinese Physical Society and IOP Publishing Ltd

carry out the present work.

In this paper, we study the linear absorption and the nonlinear dynamical properties of an EIT medium consisting of Λ-type three-level semiconductor single QDs interacting with a weak probe light and a strong coupling light field. It is found that this system exhibits a transparent window, and its width widens with the increase of control light field. Subsequently, the dynamical property of the spatial soliton is investigated in detail. We find that a weak probe light beam can form spatial weak-light dark solitons, which will transform into steady spatial weak-light ring dark solitons when it propagates along axial direction.

2. Model and linear characteristics

The self-assembled Λ-type three-level QDs system is produced in GaAs (001) substrates by molecules beam epitaxy.[34] In this experiment, the control and signal beams have linear polarizations aligned along the [110] and [1$\bar{1}$0] axes of the sample and are focused into spots of 100 μm and 20 μm in diameter respectively.[34] The average signal power is 0.02 mW; the control beam power varies between 0.05 mW and 5 mW.[34] The sample temperature changes between 5 K and 150 K.[34] According to these experimental conditions, we consider here a Λ-type three-level QDs model as shown in Fig. 1.[34] Transitions between the ground state $|0\rangle$ and state $|2\rangle$ and between states $|1\rangle$ and $|2\rangle$ are dipole-allowed while transition $|0\rangle \to |1\rangle$ is dipole-forbidden. When a strong control field is applied resonantly to the nonabsorbing transition $|1\rangle \to |2\rangle$, the quantum interference between the dipole-allowed transitions makes the normally absorbing transition $|0\rangle \to |2\rangle$ transparent. A probe field (with central angular frequency $\omega_{\rm p}$ and half Rabi frequency $\Omega_{\rm p}$) and a control field (with central angular frequency $\omega_{\rm c}$ and half Rabi frequency $\Omega_{\rm c}$) couple the transitions $|0\rangle \to |2\rangle$ and $|1\rangle \to |2\rangle$ respectively. We assume that the control field is strong and not depleted during propagation. In the interaction picture the equations of the states amplitudes and probe field can be written as

$$\left(\mathrm{i}\frac{\partial}{\partial t}+\Delta_1+\mathrm{i}\gamma_1\right)A_1+\Omega_{\rm c}^* A_2=0, \tag{1a}$$

$$\left(\mathrm{i}\frac{\partial}{\partial t}+\Delta_2+\mathrm{i}\gamma_2\right)A_2+\Omega_{\rm p}A_0+\Omega_{\rm c}A_1=0, \tag{1b}$$

$$\nabla^2 E-\frac{1}{c}\frac{\partial^2 E}{\partial t^2}-\frac{1}{\varepsilon_0 c^2}\frac{\partial^2 P}{\partial t}=0, \tag{1c}$$

where A_j is the probability of the state $|j\rangle$ $(j=0,1,2)$ satisfying the conservation condition $|A_0|^2+|A_1|^2+|A_2|^2=1$, $\Omega_{\rm c}^*$ is the conjugate of Rabi frequency $\Omega_{\rm c}$, E represents the optical field of the system, $\Delta_1=\omega_{\rm p}-\omega_{\rm c}-(\omega_1-\omega_0)$ is the two-photon detuning of the interband probe pulse with the exciton resonance, while $\Delta_2=\omega_{\rm p}-(\omega_2-\omega_0)$ is one-photon detuning, γ_j is the total decay rate of level $|j\rangle$ and has been added phenomenologically into the probability amplitude equation, $P=N_a\sum_{j=0,1}\left\{p_{j2}A_2A_j^*\exp\left[\mathrm{i}\left(k_j z-\omega_j t\right)\right]+\mathrm{c.c}\right\}$ represents the electric polarization intensity, with c.c denoting the complex conjugate and N_a, c, and ε_0 being the electron density, the light speed, and dielectric coefficient in vacuum respectively.

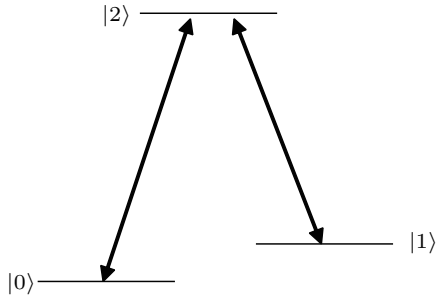


Fig. 1. Λ-type three-level self-assembled quantum dots scheme.

In the limit of weak probe field, almost all electrons will be in the ground state and we may use the steady-state approximation. The susceptibility of the probe field is

$$\begin{aligned}\chi_{\rm p} &= \frac{N\mu_{02}}{\varepsilon_0 E_{\rm p}}A_2A_0^* \\ &= \left(2c\kappa d_2/\omega_{\rm p}D\right)\left(1+W\left|\Omega_{\rm p}\right|^2\right)^{-1} \\ &= \chi_{\rm p}^{(1)}+\chi_{\rm p}^{(3)}\left|\Omega_{\rm p}\right|^2+\cdots,\end{aligned} \tag{2}$$

where $d_1=\Delta_1+\mathrm{i}\gamma_1$, $d_2=\Delta_2+\mathrm{i}\gamma_2$, $D=|\Omega_{\rm c}|^2-d_1d_2$, $W=(|\Omega_{\rm c}|^2+|d_2|^2)/|D|^2$, and $\chi_{\rm p}^{(1)}$ and $\chi_{\rm p}^{(3)}$ denote the linear susceptibility and third-order self-Kerr susceptibility of the probe field respectively. Let $\chi_{\rm p}^{(1)}={\rm Re}\chi_{\rm p}^{(1)}+\mathrm{i}{\rm Im}\chi_{\rm p}^{(1)}$, then we will have

$${\rm Re}\chi_{\rm p}^{(1)}=\frac{2c\kappa}{\omega_{\rm p}}\frac{\Delta_2\left(|\Omega_{\rm c}|^2-\Delta_1\Delta_2\right)-\Delta_1\gamma_2^2}{\left(|\Omega_{\rm c}|^2-\Delta_1\Delta_2+\gamma_1\gamma_2\right)^2+\left(\Delta_1\gamma_2+\Delta_2\gamma_1\right)^2}, \tag{3a}$$

$${\rm Im}\chi_{\rm p}^{(1)}=\frac{2c\kappa}{\omega_{\rm p}}\frac{\gamma_2\left(|\Omega_{\rm c}|^2+\gamma_1\gamma_2\right)+\Delta_2^2\gamma_1}{\left(|\Omega_{\rm c}|^2-\Delta_1\Delta_2+\gamma_1\gamma_2\right)^2+\left(\Delta_1\gamma_2+\Delta_2\gamma_1\right)^2}. \tag{3b}$$

In fact, ${\rm Im}\chi_{\rm p}^{(1)}$ and ${\rm Re}\chi_{\rm p}^{(1)}$ characterize the linear absorption coefficients of the probe field and linear refractive index respectively.

According to the experimental parameters of the self-assembled Λ-type three-level QDs,[34] we here choice $\kappa=0.0366$ cm^{-1}·meV, $\hbar\omega_{10}\approx 1.6$ eV, $\gamma_1=66$ μeV, and $\gamma_2=10^{-4}\gamma_1$. Figure 2 shows variations of ${\rm Im}\chi_{\rm p}^{(1)}$ with Δ_1/γ_1 for different strengths of the control field. It can be seen from the figure that in the absence of the control field, only a Lorentz line-sharp absorption peak appears [see the solid curve of Fig. 2]. This implies that the absorption of the probe field is maximum near the central frequency of the probe field. The

contrary case is in the presence of the control field. When the strength of the control field is rather weak, the absorption profile [see the dashed curve of Fig. 2] splits into two separate peaks, meanwhile, a deep dip on the optical absorption line can be produced. In this case, the absorption of the probe field is largely suppressed. With increasing the strength of the control field, such as the strength $\Omega_c = 0.4$ meV [see the dotted curve of Fig. 2], the dip becomes a transparent window. This phenomenon is similar to the EIT phenomenon in the atomic system. So, we can conclude that this system exhibits the EIT phenomenon. By comparing the dashed line and the dotted line, it is easy to conclude that the width of the transparent window increases as the strength of the control field increases.

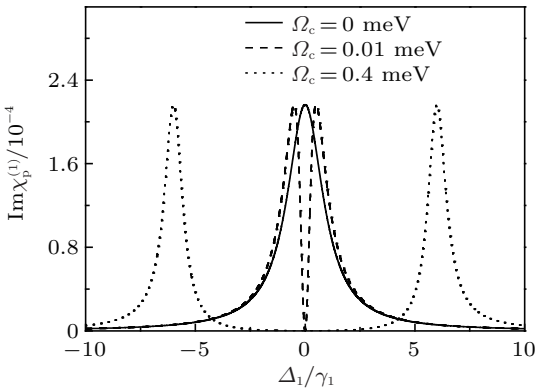


Fig. 2. Variations of linear absorption $\mathrm{Im}\chi_p^{(1)}$ with detuning Δ_1/γ_1 for the different strengths of the control field. The solid, dashed, and dotted curves correspond to the strength $\Omega_c = 0$ meV, 0.01 meV, and 0.4 meV respectively. The other parameters used are $\hbar\omega_{10} \approx 1.6$ eV, $\gamma_1 = 66$ μeV, $\gamma_2 = 10^{-4}\gamma_1$, $\kappa = 0.0366$ cm^{-1}·meV, and $\Delta_2 = 0$.

3. Spatial light solitons characteristics

In the conventional nonlinear medium, the interaction between optical and atoms is described by density matrix equation. For EIT medium, the density matrix equation can be replaced by the probability density equation.[35] And the coupling field is usually regarded as a constant[6] because it varies slowly with time. So, the time-derivative terms in Eq. (1) can be safely neglected. We obtain the following nonlinear Schrödinger (NLS) equation:

$$\mathrm{i}\frac{\partial\Omega_P}{\partial z} + \frac{c}{2\omega_p}\left(\frac{\partial^2}{\partial r^2} + \frac{1}{r}\frac{\partial}{\partial r}\right)\Omega_p + \kappa\frac{d_2\Omega_p}{D(1+W\left|\Omega_p\right|^2)} = 0, \quad (4)$$

where $\kappa = N_a\omega_p\left|p_{02}\right|^2/2\hbar\varepsilon_0 c$, and $r = \sqrt{x^2+y^2}$. For a weak probe pulse field, by expanding the last term on the left-hand side in Eq. (4) around $\left|\Omega_p\right|^2 = 0$ and introducing the dimensionless parameters $s = L_{\mathrm{diff}}^{-1}z$, $R = R_\perp^{-1}r$, and $u = \Omega_p/\Omega_0$ (where $L_{\mathrm{diff}} = \omega_p R^2/c$, $R_\perp^{-1}$, and $\Omega_0 = 1/\sqrt{W}$ represent the characteristic diffraction length, the beam radius, and the typical Rabi frequency of the probe field respectively), a dimensionless NLS equation can be given by

$$\mathrm{i}\frac{\partial u}{\partial s} + \frac{1}{2}\left(\frac{\partial^2}{\partial R^2} + \frac{1}{R}\frac{\partial}{\partial R}\right)u + a\left(1-|u|^2\right)u = 0, \quad (5)$$

where $a = \kappa d_1 L_{\mathrm{diff}}/D$. According to the realistic parameters of the self-assembled Λ-type three-level QDs,[34] we choose $\gamma_1 \approx 66$ μeV, $\gamma_2 \approx 10^{-4}\gamma_1$, $\kappa = 0.0366$ meV·cm^{-1}, $\Omega_c = 1.0$ meV, $\Delta_1 = 0.1$ meV, and $\Delta_2 = 0.4$ meV. It is easy to conclude that the imaginary part of the coefficient a is much less than its real part, so the absorption of the probe field can be safely neglected. In what follows, we preserve only the real part of the coefficient a.

Subsequently, we set $u = A(s,R)\exp[\mathrm{i}\varphi(s,R)]$. Substituting it into Eq. (5) and then separating the real part from the imaginary part, we have

$$-A\frac{\partial\varphi}{\partial s} + \frac{1}{2}\frac{\partial^2 A}{\partial R^2} - \frac{A}{2}\left(\frac{\partial\varphi}{\partial R}\right)^2 + \frac{1}{2R}\frac{\partial A}{\partial R} + aA - aA^3 = 0, \quad (6)$$

and

$$\frac{\partial A}{\partial s} + \frac{\partial A}{\partial R}\frac{\partial\varphi}{\partial R} + \frac{A}{2}\frac{\partial^2\varphi}{\partial R^2} + A\frac{1}{2R}\frac{\partial\varphi}{\partial R} = 0. \quad (7)$$

Since the above equation is nonintegrable, its analytical solutions cannot be obtained directly. Here we introduce a multiple-scale method[36–38] to make an asymptotic expansions, i.e., $A = 1 + b(\xi,\tau) = 1 + \varepsilon^2 b_0(\xi,\tau) + \varepsilon^4 b_1(\xi,\tau) + \cdots$ and $\varphi = -s + \varphi(\xi,\tau) = -s + \varepsilon\varphi_0(\xi,\tau) + \varepsilon^3\varphi_1(\xi,\tau) + \cdots$, where ε is a small parameter characterizing the relative amplitude. Slow variables $\xi = \varepsilon(R - Cs)$ and $\tau = \varepsilon^3 s$ characterize the evolution of optical soliton, with C being the dimensionless velocity. Substituting them into Eqs. (6) and (7), and separating them from each order in terms of ε respectively, from Eq. (6) we have

$$2ab_0 - C\frac{\partial\varphi_0}{\partial\xi} = 0, \quad (8)$$

$$2ab_1 - C\frac{\partial\varphi_1}{\partial\xi} = b_0 C\frac{\partial\varphi_0}{\partial\xi} - \frac{\partial\varphi_0}{\partial\tau} - \frac{1}{2}\left(\frac{\partial\varphi_0}{\partial\xi}\right)^2 + \frac{1}{2}\frac{\partial^2 b_0}{\partial\xi^2} - 3ab_0^2, \quad (9)$$

and from Eq. (7), we have

$$C\frac{\partial b_0}{\partial\xi} - \frac{1}{2}\frac{\partial^2\varphi_0}{\partial\xi^2} = 0, \quad (10)$$

$$C\frac{\partial b_1}{\partial\xi} - \frac{1}{2}\frac{\partial^2\varphi_1}{\partial\xi^2} = \frac{b_0}{2}\frac{\partial^2\varphi_0}{\partial\xi^2} + \frac{1}{2C\tau}\frac{\partial\varphi_0}{\partial\xi} + \frac{\partial b_0}{\partial\tau} + \frac{\partial b_0}{\partial\xi}\frac{\partial\varphi_0}{\partial\xi}. \quad (11)$$

By comparing Eq. (8) with Eq. (10), we find $C^2 = a$. Similarly, by comparing Eq. (9) with Eq. (11), we obtain

$$8C\frac{\partial b_0}{\partial\tau} + 24ab_0\frac{\partial b_0}{\partial\xi} - \frac{\partial^3 b_0}{\partial\xi^3} + \frac{4C}{\tau}b_0 = 0. \quad (12)$$

Setting $w = \varepsilon^2 b_0$, and using the transformations $\xi = \varepsilon(R - Cs) = \varepsilon R'$ and $\tau = \varepsilon^3 s$, one has

$$\frac{\partial w}{\partial s} + 3Cw\frac{\partial w}{\partial R'} - \frac{1}{8C}\frac{\partial^3 w}{\partial R'^3} + \frac{1}{2s}w = 0. \quad (13)$$

To our knowledge, this equation is a typical cylindrical Korteweg-de Vries equation, of which the single soliton solution reads[37]

$$w = k(s)\mathrm{sech}^2\{\lambda(s)[R' - \beta(s)]\}. \tag{14}$$

Here, $k = k_0 \exp[-2\ln(s+s_0)/3]$ is the amplitude of the soliton, where k_0 and s_0 correspond to the initial amplitude and the initial axial position of the soliton respectively.

$$\lambda = C\sqrt{-2k_0 \exp[-2\ln(s+s_0)/3]}$$

is the width of the soliton, and

$$\beta = 3sCk_0 \exp[-2\ln(s+s_0)/3] + l,$$

where l is a real constant.

To verify the stability of the soliton solutions, we carry out numerical simulations of Eq. (14) with a small perturbation initially implanted to see whether the propagation is stationary. About five percent of the amplitude $k(s)$ is initially added as the perturbations. The profiles of w^2 changing with beam diffraction direction R at the different axial positions are plotted in Fig. 3. It is observed that the two-dimensional spatial optical soliton obtained is stable.[17]

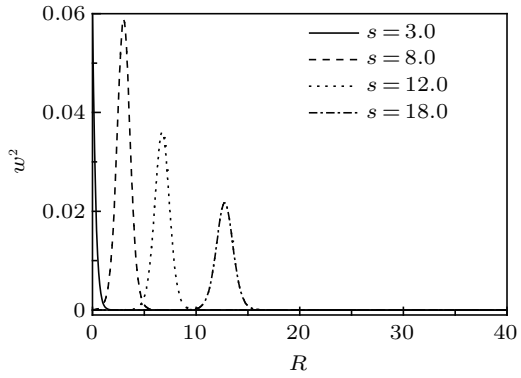


Fig. 3. Variations of w^2 with beam diffraction direction R at different axial positions. The solid, dashed, dotted, and dashed–dotted curves correspond to the strengths $s = 3.0$, 8.0, 12.0, and 18.0 respectively. The parameters used are $s_0 = 1.0$, $k_0 = -1.0$, $l = 0.0$, and $a = 1.5$.

Since the soliton may propagate stably, we then study the dynamical properties. To be exact to the first order, the soliton solution of Eq. (5) is

$$u = \{1 + k(s)\,\mathrm{sech}^2[\lambda(s)(R' - \beta(s))]\}\exp(\mathrm{i}\varphi). \tag{15}$$

In order to obtain visually the dynamical behaviors of the spatial weak-light soliton in the self-assembled Λ-type three-level QDs, we calculate the intensity distribution of the probe field along different axial positions in Fig. 4. Here $s_0 = 1.0$

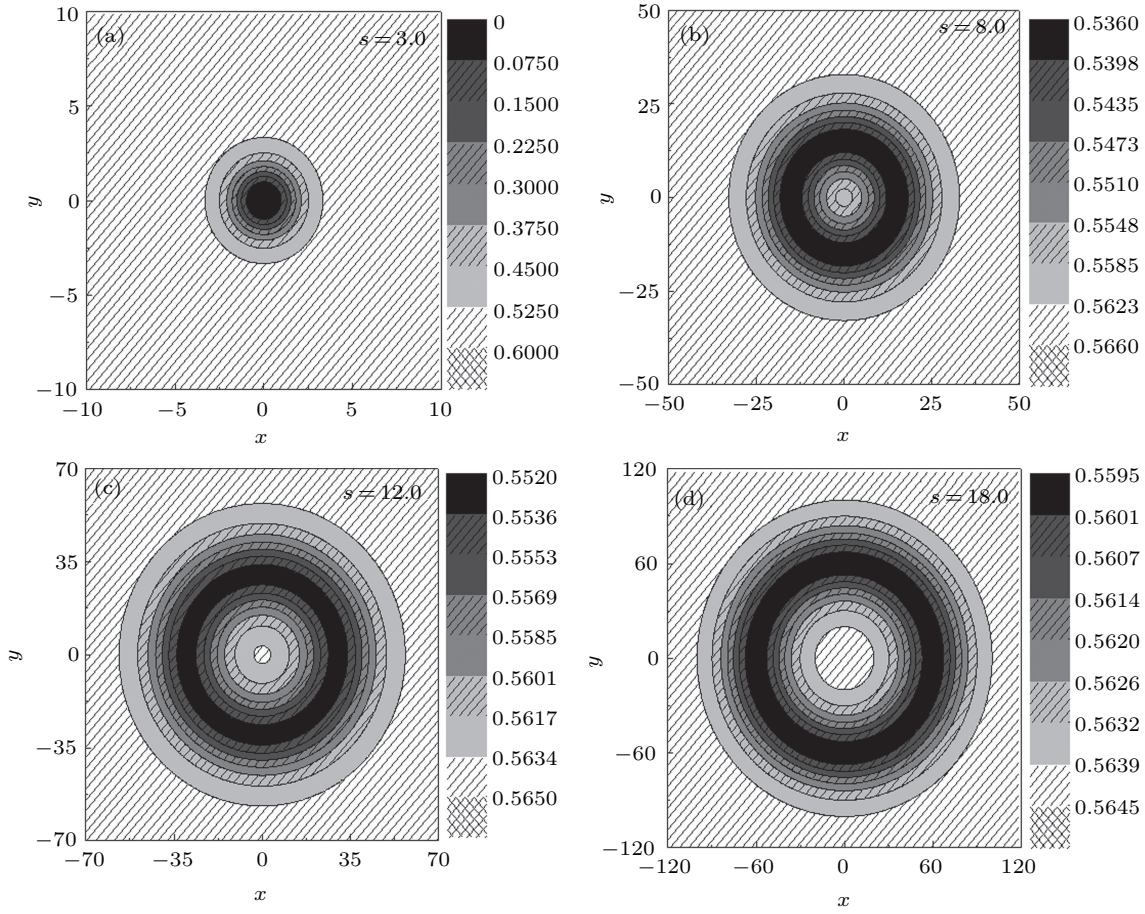


Fig. 4. Density distributions of the probe field at axial position $s = 3.0$ (a), 8.0 (b), 12.0 (c), and 18.0 (d). The parameters used are the same as those of Fig. 3.

is chosen as the initial position of the forming soliton. From Fig. 4(a), one finds that when $s = 3.0$ in the center in the plane there exists a minimum density circular macula and the minimum value of the density comes down to zero. Obviously, there is a spatial weak-light dark soliton due to the balance between the beam diffraction and refractive nonlinearly. When the soliton propagates to the axial position $s = 8.0$ [see Fig. 3(b)], the density of the circular macula in the central area is nonzero and the minimum density circular ring is away from the center of the plane. It illustrates that the spatial weak-light dark soliton transforms into a spatial weak-light ring dark soliton and it is in a growing process. For the axial position $s = 12.0$ [which is shown as Fig. 4(c)], we find that the minimum density circular ring spreads along the radial direction. Meanwhile, a platform appears in the center area, which means that the density of the center in the plane is equal to that of the background. It shows that the spatial weak-light ring dark soliton has been fully formed. When the soliton propagates at the axial position $s = 18.0$ [see Fig. 4(d)], the areas of the central platform and the ring dark soliton expand along the radial direction further. By comparing with Fig. 4(c), the width and amplitude of the ring dark soliton keep unchanged nearly, which illustrates that the ring dark soliton is dynamically stable.

4. Conclusions

In this paper, we analytically studied the optical absorption properties and the soliton characteristics in lifetime broadened Λ-type three-level self-assembled quantum dots. First, by using semi-classical theory, we derived a Maxwell–Schrödinger equation which describes the energy-level conformation of the self-assembled quantum dots. Subsequently, by solving the Maxwell–Schrödinger equation, the linear absorption of the probe field and linear refractive index were obtained. Furthermore, numerical calculations show that the linear absorption of the probe optical field is greatly suppressed. This system exhibits a transparent window, and its width widens with the increase of control light field. Finally, we studied the soliton propagation properties with a weak probe light beam, and obtained a typical cylindrical Korteweg-de Vries equation which describes the amplitude of the Rabi frequency of the probe field. By numerical calculation, it is found that a weak probe light beam can form spatial weak-light solitons. When it propagates along the axial direction, the soliton will transform into a steady spatial weak-light ring dark soltion. And the width and amplitude of the ring dark soliton keep unchanged which possesses dynamic stability. Due to the fact that the absorption of the probe field is greatly suppressed, it is sure that the spatial weak-light ring dark soliton can propagate stably without attenuation.

References

[1] Haus H A and Wong W S 1996 *Rev. Mod. Phys.* **68** 423
[2] Chen Z G, Segev M and Christodoulides D N 2012 *Rep. Prog. Phys.* **75** 86401
[3] Stegeman G I and Segev M 1998 *Phys. Today* **51** 42
[4] Hasegawa A and Kodama Y 1995 *Solitons in Optical Communications* (Oxford: Clarendon Press)
[5] Hang C, Huang G X and Deng L 2006 *Phys. Rev. E* **74** 046601
[6] Luo X Q, Wang D L, Zhang Z Q, Ding J W and Liu W M 2011 *Phys. Rev. A* **84** 033803
[7] Kang H and Zhu Y F 2003 *Phys. Rev. Lett.* **91** 093601
[8] Wang D L, Yan X H and Liu W M 2008 *Phys. Rev. E* **78** 026606
[9] Li L and Huang G X 2010 *Eur. Phys. J. D* **58** 339
[10] She Y C, Wang D L, Zhang W X, He Z M and Ding J W 2010 *J. Opt. Soc. Am. B* **27** 208
[11] Wang D L and Yan X H 2011 *Int. J. Mod. Phys. B* **25** 781
[12] Wu Y and Yang X X 2007 *Appl. Phys. Lett.* **91** 094104
[13] Hu X and Li B 2011 *Chin. Phys. B* **20** 050315
[14] Wang D L, Yan X H and Wang F J 2007 *Chin. Phys. Lett.* **24** 1817
[15] Ma Y H and Zhou L 2013 *Chin. Phys. B* **22** 024204
[16] Li B, Zhang X F, Li Y Q, Chen Y and Liu W M 2008 *Phys. Rev. A* **78** 023608
[17] Chen J C, Li B and Chen Y 2013 *Chin. Phys. B* **22** 110306
[18] Liu C F, Fan H, Gou S C and Liu W M 2014 *Sci. Rep.* **4** 4224
[19] Liu C F, Yu Y M, Gou S C and Liu W M 2013 *Phys. Rev. A* **87** 063630
[20] Hang C, Knototop V V and Huang G X 2009 *Phys. Rev. A* **79** 033826
[21] Liu C F, Fan H, Zhang Y C, Wang D S and Liu W M 2012 *Phys. Rev. A* **86** 053616
[22] Zhang X F, Hu X H, Liu X X and Liu W M 2009 *Phys. Rev. A* **79** 033630
[23] Liu C F and Liu W M 2012 *Phys. Rev. A* **86** 033602
[24] Li H J, Wu Y P and Huang G X 2011 *Phys. Rev. A* **84** 033816
[25] Li Q Y, Li Z D, Yao S F, Li L and Fu G S 2010 *Chin. Phys. B* **19** 080501
[26] Song W W, Li Q Y, Li Z D and Fu G S 2010 *Chin. Phys. B* **19** 070503
[27] Hang C and Knototop V V 2011 *Phys. Rev. A* **83** 053845
[28] Peng P C, Lin C T, Kuo H C, Tsai W K, Liu J N, Chi S, Wang S C, Lin G, Yang H P, Lin K F and Chi J Y 2006 *Opt. Express* **14** 12880
[29] Su H and Chuang S L 2006 *Opt. Lett.* **31** 271
[30] Villas B J M, Govorov A O and Ulloa S E 2004 *Phys. Rev. B* **69** 125342
[31] Yang W X, Chen A X, Lee R K and Wu Y 2011 *Phys. Rev. A* **84** 013835
[32] She Y C, Zheng X J, Wang D L and Zhang W X 2013 *Opt. Express* **21** 17392
[33] Li J H, Yu R, Huang P and Yang X X 2009 *Phys. Lett. A* **373** 554
[34] Marcinkevičius S, Gushterov A and Reithmaier J P 2008 *Appl. Phys. Lett.* **92** 041113
[35] Dutton Z 2002 Ph. D. Thesis (Harvard University)
[36] Huang G X, Deng L and Payne M G 2005 *Phys. Rev. E* **72** 016617
[37] She Y C, Wang D L and Ding J W 2009 *Acta Phys. Sin.* **58** 3198 (in Chinese)
[38] Zeng K H, Wang D L, She Y C and Zhang W X 2013 *Acta Phys. Sin.* **62** 147801 (in Chinese)